64375-RG-RV-3

SUPPLEMENTAL INFORMATION

Improved regenerative myogenesis and muscular dystrophy in mice lacking MKP-5

Hao Shi[1], Mayank Verma[1], Lei Zhang[1], Chen Dong[3], Richard A. Flavell[4]

and Anton M. Bennett[1, 2]

[1]Department of Pharmacology and [2]Program in Integrative Cell Signaling and Neurobiology of Metabolism, Yale University School of Medicine, New Haven, CT 06520, United States

[3]Department of Immunology, The University of Texas MD Anderson Cancer Center, Houston, TX

[4]Department of Immunobiology and Howard Hughes Medical Institute, Yale University School of Medicine, New Heaven, CT 06520, United States

Contents:

Correspondence to:
Anton M. Bennett, Ph.D.
Yale University School of Medicine
Department of Pharmacology
SHM B226D
333 Cedar Street
New Haven, CT 06520-8066, USA
E-mail: anton.bennett@yale.edu
Phone: 1-203-737-2441
Fax: 1-203-737-2738

Online methods

Cytokine measurements. *mkp-5*$^{+/+}$ and *mkp-5*$^{-/-}$ mice were injected with cardiotoxin, 2d later, muscles were harvested and protein extracts were subjected to cytokine measurement using the mouse cytokine/chemokine MILLIPLEX MAP Kit (Millipore). Cytokine levels were normalized to total protein for the 96-well plate assay.

Immunohistochemical staining of Pax7. Pax7 antibody was purchased from the Developmental Study Hybridoma Bank. Nuclei were stained with TO-PRO-3 (blue). Pax7 antibody stained Pax7 (green, with FITC-conjugated secondary antibody) and non-specifically stained red blood cells (no nuclei). In merged images, Pax7 positive satellite cells were cyan (containing nuclei), whereas the red blood cells remained green (no nuclei).

Immunoblotting. Muscles collected from the non-damaged or CTX damaged muscles were pulverized in liquid nitrogen before being homogenized in RIPA lysis buffer. Equal amount of protein was loaded and separated by 10% SDS-PAGE gel. Cyclin D1, cyclin D2, cyclin D3, CDK4, CDK6, p15, pRb, Rb, p-c-Jun, c-Jun, pAkt, pS6K1, and p53 antibodies were bought from Cell Signaling Tech, ERK1/2, Akt, and S6K1 antibodies were from Santa Cruz Biotech. For densitometric analysis of the immunoblots, blots were scanned using CanoScan LiDE 100 scanner and the densitometry was analyzed using LabWorks Image Acquisition and Analysis software.

Cytokines	Concentration (pg/g protein)	
	mkp-5$^{+/+}$	*mkp-5*$^{-/-}$
GM-CSF	1103±116	1147±140
IFNγ	693±192	10103±1166*
IL-1β	3445±814	3010±615
IL-4	263±57	203±27
IL-6	4746±1686	14363±3332*
IL-10	279±67	361±86
TNFα	703±133	798±189

Supplemental Table 1

Cytokine levels in 2-day cardiotoxin (CTX)-damaged skeletal muscles. Data represents the mean ± S.E.M. and were generated from 8-week-old male *mkp-5*$^{+/+}$ and *mkp-5*$^{-/-}$ mice. The levels of the indicated cytokines were undetectable in undamaged skeletal muscles of *mkp-5*$^{+/+}$ and *mkp-5*$^{-/-}$ mice. Data represent means ± S.E.M. from n=9-10 mice. *; $P<0.05$.

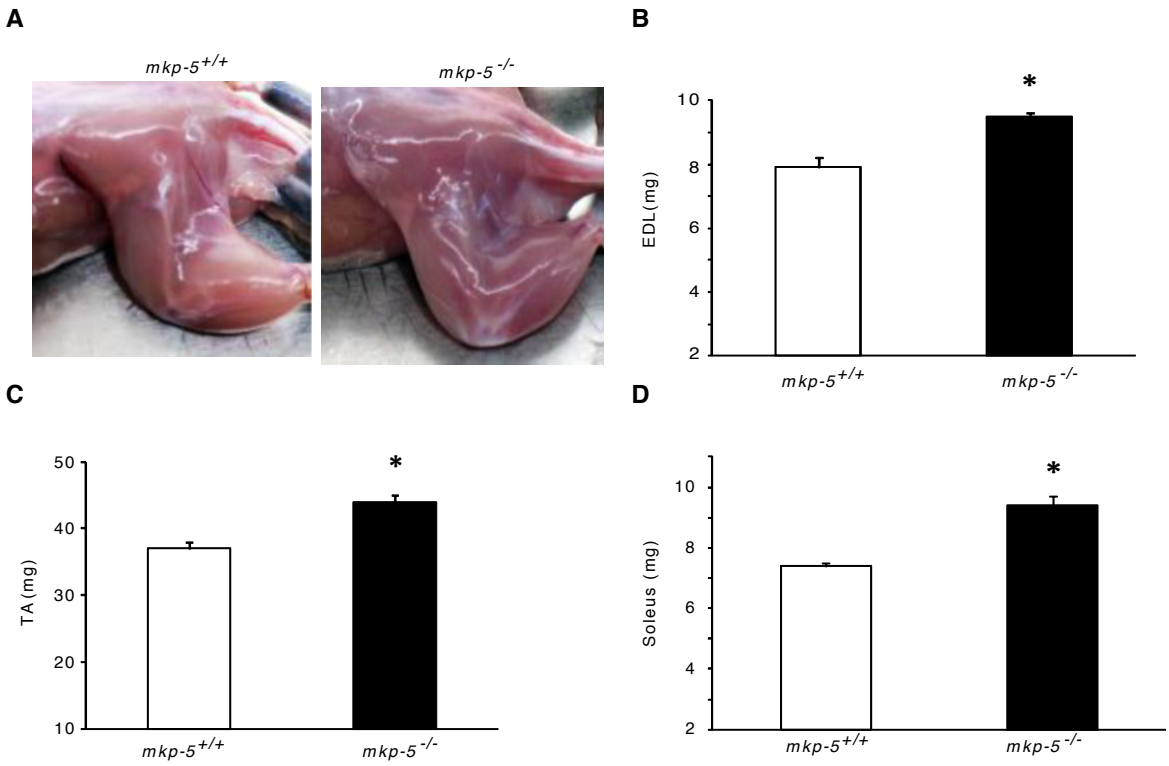

Supplemental Figure 1

MKP-5-deficiency increases skeletal muscle mass. (**A**) Representative images from the hind limb muscles of *mkp-5*$^{+/+}$ and *mkp-5*$^{-/-}$ mice. (**B-D**), muscle mass of extensor digitorum longus (EDL, **B**), tibialis anterior (TA, **C**), and soleus (**D**) muscles from at least 5 littermates. Histograms represent mean ± S.E.M. and data was generated from 8-week-old male mice. *; $P<0.05$ compared with *mkp-5*$^{+/+}$ muscles.

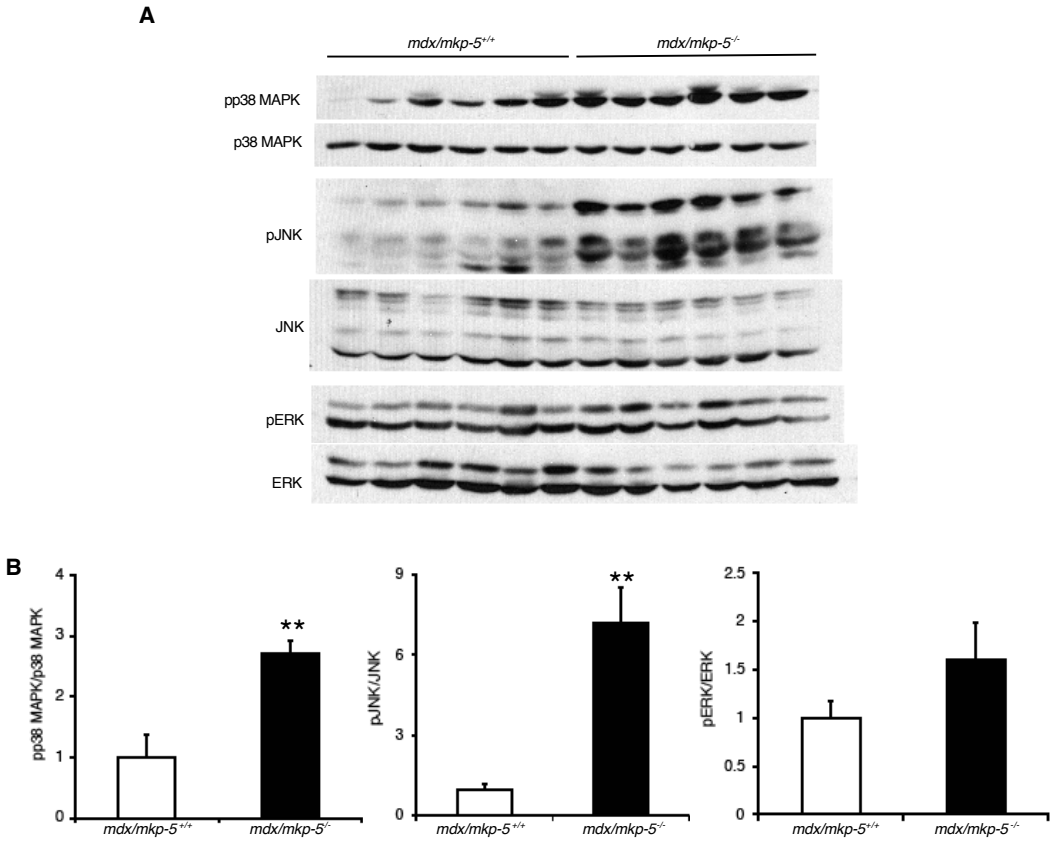

Supplemental Figure 2

MKP-5 antagonizes p38 MAPK and JNK in *mdx* mice. (**A**) Muscle homogenates from *mdx*/*mkp-5*$^{+/+}$ and *mdx/mkp-5*$^{-/-}$ mice were prepared. Lysates were immunoblotted for phosphorylated p38 MAPK, JNK and ERK1/2 and total corresponding MAPKs. n=6 per genotype. (**B**) Quantitation of the immunoblots from (A). Histogram represents the mean ± S.E.M. Data were generated from 3-month-old males. **; $P < 0.01$ compared with *mdx*/*mkp-5*$^{+/+}$ mice.

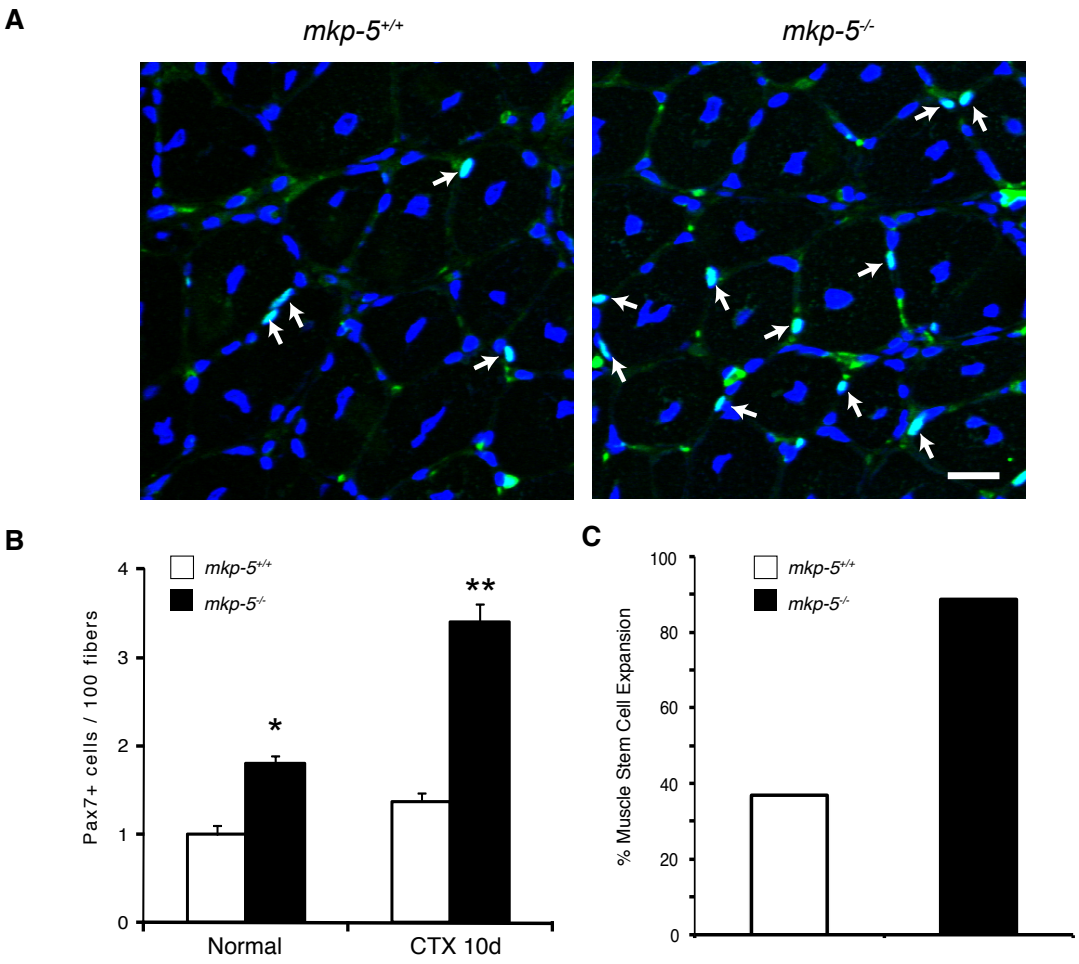

Supplemental Figure 3

Enumeration of Pax7-positive satellite cells. (**A**) Immunofluorescence staining of Pax 7 in 10d CTX-damaged soleus muscle. Cyan, Pax7; Blue, nuclei; Green, non-specific staining. Scale bar, 20 μm. Non-specifically stained green cells are red blood cells. (**B**) $Pax7^+$ cells per 100 muscle fibers were counted in normal, non-damaged muscles and 10d post CTX-damaged muscle cross-sections. (**C**) % Muscle stem cell expansion represented as the percentage increase in $Pax7^+$ cells derived from **B**. Histograms represent the mean ± S.E.M. n=6 per genotype for each treatment. Data were generated from 8-week-old male mice. *; $P<0.05$, ** $P<0.01$ compared with *mkp-5*$^{+/+}$ mice.

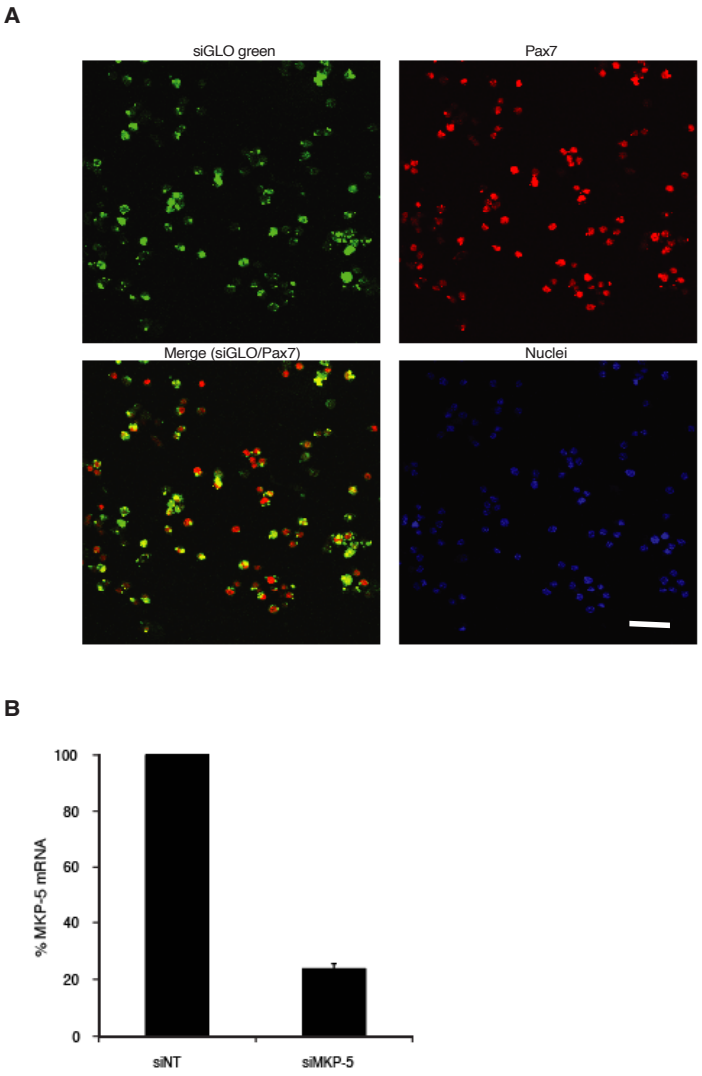

Supplemental Figure 4

MKP-5 knockdown in satellite cell-derived myoblasts. Satellite cell (SC)-derived myoblasts were isolated from 8-week-old male C57BL/6J mice and cultured in F-10 containing 20% FBS. (**A**) SC-derived myoblasts were transfected with siGLO Green using Lipofectamine 2000. 24h later, confocal images were taken to assay for transfection efficiency. Scale bar, 50 μm. (**B**) SC-derived myoblasts were transfected with either non-targeting siRNA (siNT) or MKP-5 siRNA (siMKP-5), cells were harvested 48h later, MKP-5 mRNA was assayed by quantitative RT-PCR and expressed as percent control. Histogram represents three independent experiments with 3 replicates in each.

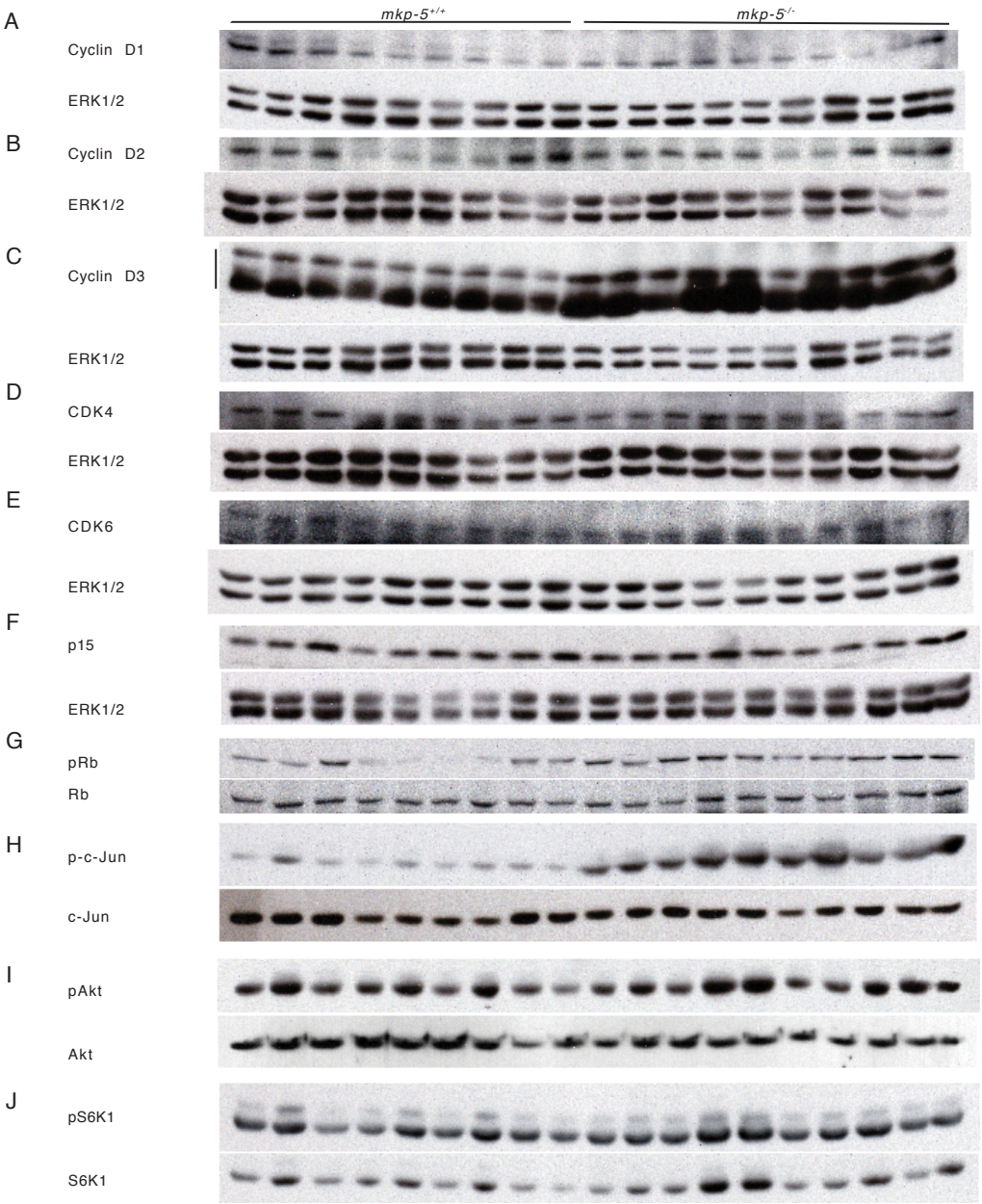

Supplemental Figure 5

Expression levels of cell cycle regulators and signaling proteins 2d after muscle damage. Tibialis anterior muscle lysates from *mkp-5*$^{+/+}$ and *mkp-5*$^{-/-}$ mice were separated by 10% SDS-PAGE and immunoblotted with the antibodies as indicated (**A - J**). Each lane represents an individual mouse from n=9 *mkp-5*$^{+/+}$ and n=10 *mkp-5*$^{-/-}$ mice.

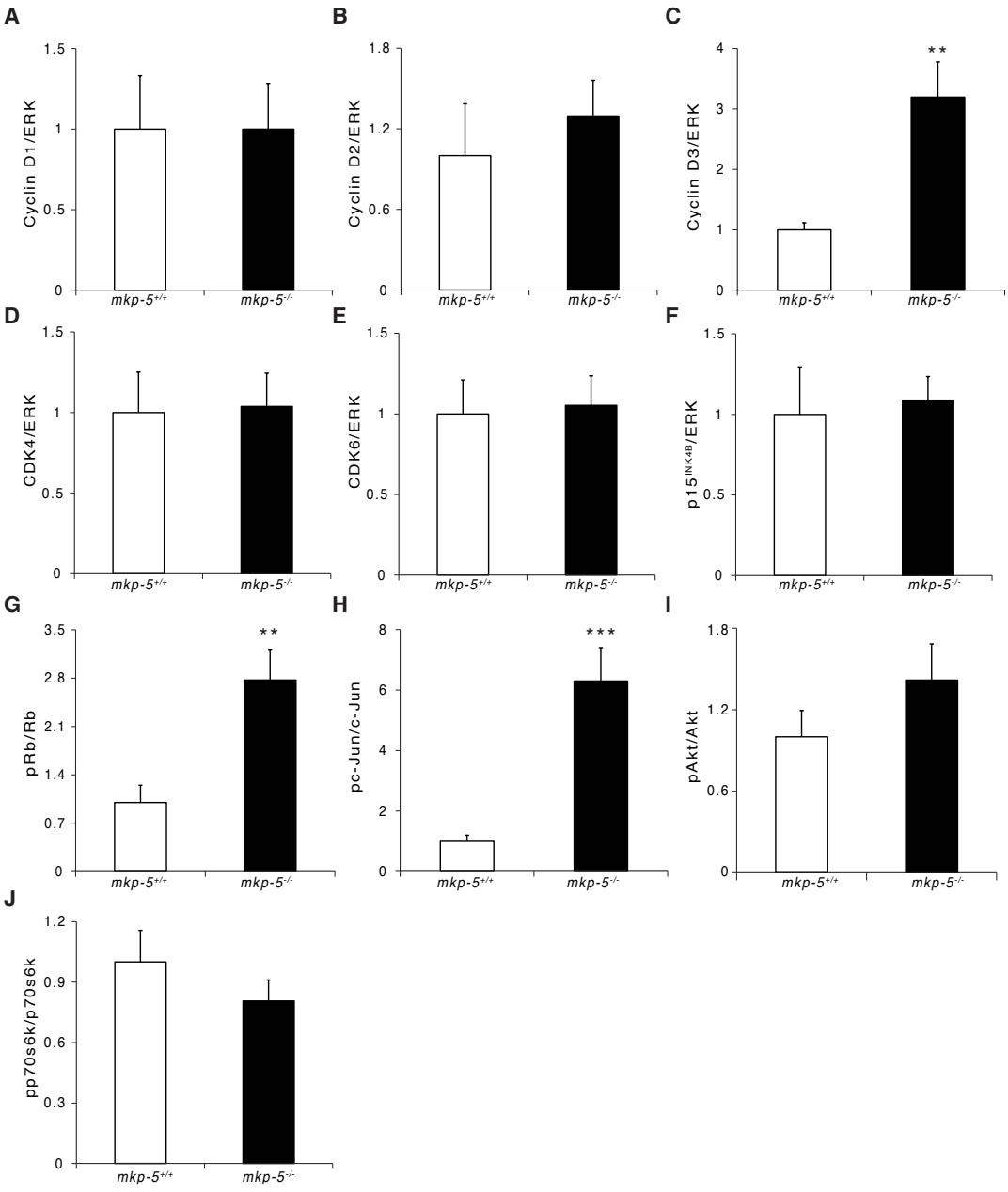

Supplemental Figure 6

Quantitation of expression levels of cell cycle regulators and signaling proteins 2d after muscle damage from Supplemental Figure 5 (**A-J**). The histograms represent the mean ± S.E.M. relative densitometric values from immunoblots derived from *mkp-5*$^{+/+}$ and *mkp-5*$^{-/-}$ mice. n=9 *mkp-5*$^{+/+}$ and n=10 *mkp-5*$^{-/-}$ mice. **; P<0.01, ***; P<0.001 compared with *mkp-5*$^{+/+}$.

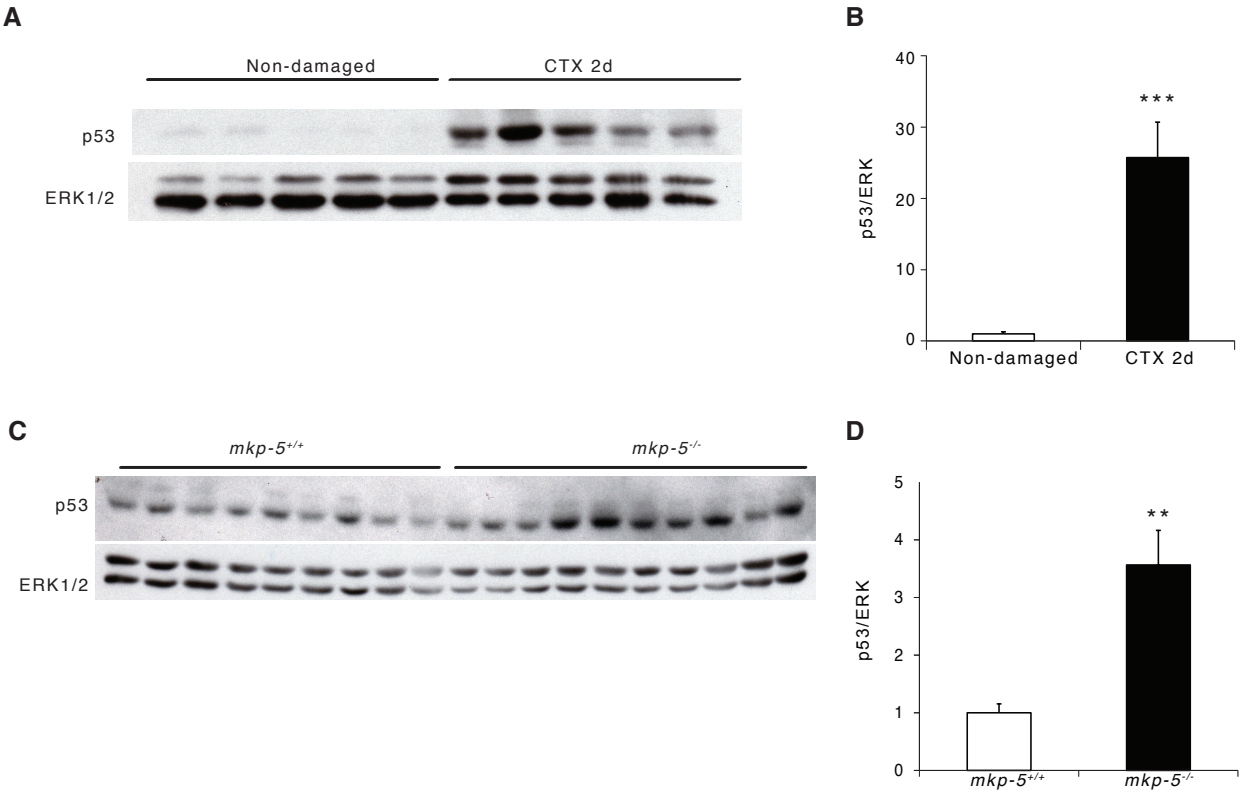

Supplemental Figure 7

Changes in p53 expression in non-damaged and CTX-damaged muscles from *mkp-5*$^{+/+}$ and *mkp-5*$^{-/-}$ mice. (**A**) Skeletal muscle lysates prepared from non-damaged and CTX-damaged 8-week-old male C57BL/6J mice were immunoblotted for the expression of p53 and ERK1/2 (**B**) Densitometric quantitation of immunoblots shown in (A). Histogram represents mean ± S.E.M. from n=5 mice per treatment group. (**C**) 2d CTX-damaged muscle lysates from 8-week-old male *mkp-5*$^{+/+}$ and *mkp-5*$^{-/-}$ mice were blotted with antibodies against p53 and ERK1/2. (**D**) Densitometric quantitation of immunoblots shown in (C). Histogram represents mean ± S.E.M. from n=9 *mkp-5*$^{+/+}$ and n=10 *mkp-5*$^{-/-}$ mice. **; P<0.01; ***; P<0.001 compared with the corresponding controls.

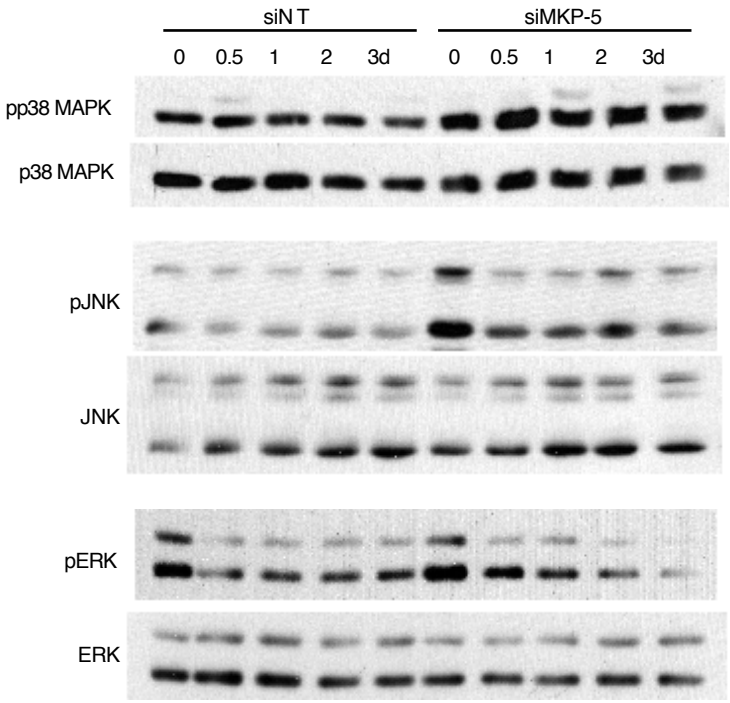

Supplemental Figure 8

MKP-5 antagonizes p38 MAPK and JNK during myogenesis. Non-targeting (NT) and MKP-5 siRNAs were transfected into C2C12 myoblasts and myoblasts were differentiated for 3d. Cell lysates were analyzed for phosphorylated and total p38 MAPK, JNK and ERK expression by immunoblotting. Data are representative of three independent experiments.